Journal of the Physical Society of Japan **81** (2012) 084001 **FULL PAPERS**
http://dx.doi.org/10.1143/JPSJ.81.084001

# Rogue Waves for the Coupled Schrödinger–Boussinesq Equation and the Coupled Higgs Equation

Gui MU[1] and Zhenyun QIN[2,3*]

[1]*College of Mathematics and Information Science, Qujing Normal University, Qujing 655011, P. R. China*
[2]*School of Mathematics and LMNS, Fudan University, Shanghai 200433, P. R. China*
[3]*Department of Mathematics, University of Michigan, Ann Arbor, MI 48109, U.S.A.*

(Received May 7, 2012; accepted June 7, 2012; published online July 13, 2012)

In this work, firstly it is shown that the coupled Schrödinger–Boussinesq equation, which governs the nonlinear propagation of coupled Langmuir and dust-acoustec wave in a multicomponent dusty plasma, possesses rogue waves in the form of the rational solutions. Here a hierarchy of rational solutions, the Peregrine breather and the second-order rational solution are given by means of the Hirota technique. Also, it is worth noting that the electric field exhibits bright rogue wave feature while electrostatic potential plays a role of dark rogue wave. Meanwhile, in comparison with rogue wave of nonlinear Schrödinger equation, some novel features of rogue waves are presented in their second order rational solutions. Secondly, rational solution of the coupled Higgs equation is taken into account by utilizing Hirota technique and the existence condition of rogue wave for this system is discussed.

KEYWORDS: Rogue wave, Schrödinger–Boussinesq equation, coupled Higgs equation, Hirota technique

## 1. Introduction

In recent years the term "Rogue waves" has been triggered much interest in various physical branches[1–9] although there is no exact definition up to now. A possible mechanism for the formation of rogue waves is associated with modulation instability.[10–14] The mysteriousness of rogue wave events mainly lies in the phenomenon which appears out of nowhere and disappears without trace. As is known, the Peregrine breather (PB),[10] whose representation is mathematically a ratio of two polynomials, can be used to describe this feature because it is a spatially localized breather with only one oscillation in time within the framework of the classic "focusing" nonlinear Schrödinger equation (NLSE).[15] It can be also considered as a limiting cases of either periodic "Ma solitons"[16] (MS) or "Akhmediev breathers"[17] (ABs). In particular, it is the lowest-order rational solution in the whole hierarchy of NLSE.[18–20] Experimentally it is observed in 2010 by making use of modulational instability of continuous wave.[21]

In this work, firstly Schrödinger–Boussinesq (SB) equation is considered

$$\begin{aligned} &\mathrm{i}E_t + E_{xx} + \beta_1 E - NE = 0, \\ &3N_{tt} - N_{xxxx} + 3(N^2)_{xx} + \beta_2 N_{xx} - (|E|^2)_{xx} = 0, \end{aligned} \tag{1}$$

where $\beta_1$ and $\beta_2$ are real constants, $E(x,t)$ is a complex function and $N(x,t)$ is a real function. This system (1) is known to describe the nonlinear propagation of coupled Langmuir and dust-acoustec wave in a multicomponent dusty plasma.[22] Hase and Satsuma have obtained $N$-soliton solution of SB system.[23] The complete integrability of system (1) has been studied from the view of Painlevé analysis.[24] Homoclinic solution of eq. (1) has been presented by Hu etc. by employing Hirota method.[25] Secondly, the coupled Higgs equaiton reads

$$\begin{aligned} &U_{tt} - U_{xx} - \alpha U + \beta U|U|^2 - 2UV = 0, \\ &V_{tt} + V_{xx} - \beta(|U|^2)_{xx} = 0. \end{aligned} \tag{2}$$

This model describes a system of conserved scalar nucleons interacting with neutral scalar mesons. Here, the function $V = V(x,t)$ represents a real scalar meson field and $U = U(x,t)$ a complex scalar nucleon field. It is the coupled nonlinear Klein–Gordon equation for $\alpha < 0, \beta < 0$ and the coupled Higgs field equation for $\alpha > 0, \beta > 0$. The homoclinic orbit[25] and the existence of $N$-soliton solutions[26] for eq. (2) have been shown by the Hirota bilinear method. The coupled nonlinear Klein–Gordon equation exhibits the feature of breather resonance.[27] Painlevé integrability of eq. (2) has been shown.[28] The purpose is to devote to carrying out a hierarchy of rational solutions, the PB and the second-order rational solution of eqs. (1) and (2) by means of the Hirota technique.

The structure of the work is organized as follows. In §2, various species of exact solutions of eq. (1) are constructed, such as ABs, MS, PB, and the second-order rational solutions. In §3, the rational solution of eq. (2) is examined and the existence condition of rogue wave is analyzed from its explicit expression. The conclusion is drawn in §4.

## 2. Schrödinger–Boussinesq Equation

In this section, we focus on constructing various kinds of exact solutions of eq. (1). Plugging the Bäcklund transformation into eq. (1):

$$\begin{aligned} E(x,t) &= \frac{g(x,t)}{f(x,t)}, \\ N(x,t) &= -2[\ln(f(x,t))]_{xx}, \end{aligned} \tag{3}$$

where $g(x,t)$ is an unknown complex function and $f(x,t)$ is a real function. One can find the bilinear form of SB equation (1):

$$\begin{aligned} &(D_x^4 - 3D_t^2 - \beta_2 D_x^2 - A)f \cdot f - g^* g = 0, \\ &(\mathrm{i}D_t + D_x^2 + \beta_1)g \cdot f = 0, \end{aligned} \tag{4}$$

where $g^*$ is conjugate function of $g(x,t)$, A is the integration constant and the $D$-operator is defined by

$$\begin{aligned} &D_x^m D_t^n f(x,t) \cdot g(x,t) \\ &= \left(\frac{\partial}{\partial x} - \frac{\partial}{\partial x'}\right)^m \left(\frac{\partial}{\partial t} - \frac{\partial}{\partial t'}\right)^n [f(x,t)g(x',t')]|_{x'=x,t'=t}. \end{aligned}$$

*E-mail: zyqin@fudan.edu.cn

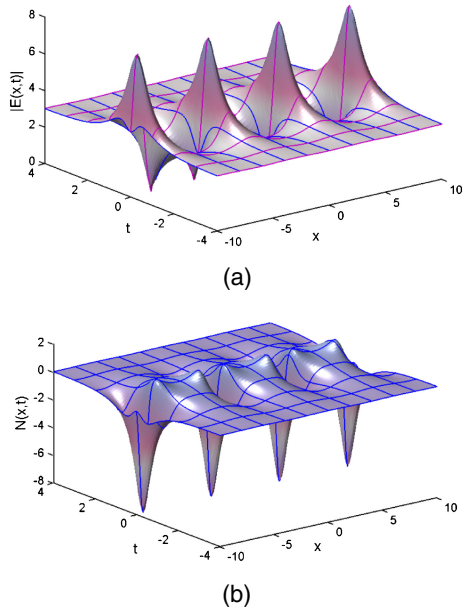


**Fig. 1.** (Color online) Evolution of electric $E(x,t)$ (a) and electrostatic potential $N(x,t)$ (b) for $\beta = 0.8$, $k = 1$, $\beta_2 = -2$, and $\beta_1 = 1$ in "Akhmediev breather" eqs. (5) and (6).

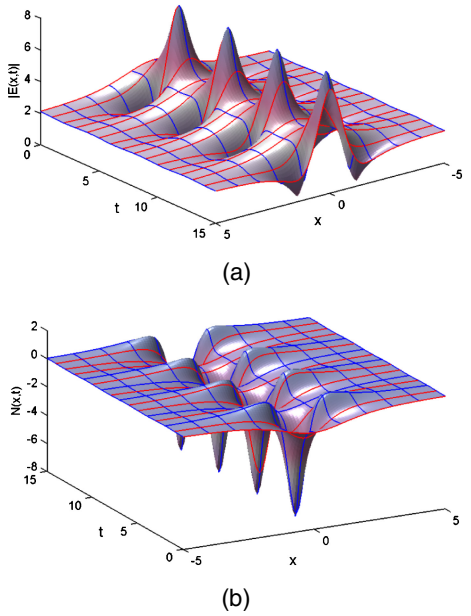


**Fig. 2.** (Color online) Evolution of electric $E(x,t)$ (a) and electrostatic potential $N(x,t)$ (b) for $k = 1.5$, $c = 1$, $\beta_1 = 1$, and $\beta_2 = 1$ in "Ma soliton" eqs. (8) and (9).

### 2.1 ABs

Here we construct the ABs type of SB equation with the help of its bilinear form. ABs is associated with modulation instability and is space-periodic and time localized which approaches the plane wave $(E, N) = (e^{i\beta_1 t}, 0)$ as $t \to \infty$.[17] Through the long and tedious calculation, a family solution of ABs of SB equation (1) reads as follows:

$$E(x,t) = a e^{i\beta_1 t} \frac{(2\beta^2 - 1)\cosh(\alpha t) + \beta\cos(kx) + i2\beta\sqrt{1-\beta^2}\sinh(\alpha t)}{\cosh(\alpha t) + \beta\cos(kx)}, \tag{5}$$

$$N(x,t) = \frac{2\beta k^2\{\cos(kx)[\cosh(\alpha t) + \beta\cos(kx)] + \beta\sin^2(kx)\}}{[\cosh(\alpha t) + \beta\cos(kx)]^2}, \tag{6}$$

where

$$a = \frac{k[k^2(4\beta^2 - 1) + \beta_2(\beta^2 - 1)]^{1/2}}{\sqrt{2}(\beta^2 - 1)}, \quad \alpha = \beta k^2(1-\beta^2)^{-1/2}. \tag{7}$$

From eq. (7), this family of solutions is valid when two free parameters $\beta$ and $k$ should satisfy $0 < \beta^2 < 1$ and $k^2(4\beta^2 - 1) + \beta_2(\beta^2 - 1) > 0$. We note that the period of this solution is equal to $2\pi/k$. When the period tends to infinity, the parameters $a$ and $\alpha$ will become zero. Then, when $k \to 0$, the amplitudes of the solutions $E(x,t)$ and $N(x,t)$ in eqs. (5) and (6) will be zero. On the other hand, if $\alpha > 0$, we found $E \to a e^{i\beta_1 t}(2\beta^2 - 1 + i2\beta\sqrt{1-\beta^2})$, $N \to 0$ as $t \to \infty$ and $E \to a e^{i\beta_1 t}(2\beta^2 - 1 - i2\beta\sqrt{1-\beta^2})$, $N \to 0$ as $t \to -\infty$. It is shown that the solution given by eqs. (5) and (6) also represents a heteroclinic solution of SB equation. An example of this solution is plotted in Fig. 1 with the values of parameters $\beta = 0.8$, $k = 1$, $\beta_2 = -2$, and $\beta_1 = 1$.

### 2.2 MS

Also there exists the other breather-type solution for NLSE which breathes temporally and tends to the plane wave solution as $x \to \infty$ but is spatially localized which is found by Ma.[16] Here, we also want to construct this MS type solution of eq. (1) using its bilinear form. The MS solution of eq. (1) is produced:

$$E(x,t) = e^{i\beta_1 t} \frac{2k\alpha^2\cosh(cx) + \sqrt{k^2 - c^4}[\beta\cos(kt) + i\gamma\sin(kt)]}{2c^2\alpha[k\cosh(cx) + \sqrt{k^2 - c^4}\cos(kt)]}, \tag{8}$$

$$N(x,t) = \frac{-2kc^2[k + \sqrt{k^2 - c^4}\cosh(cx)\cos(kt)]}{[k\cosh(cx) + \sqrt{k^2 - c^4}\cos(kt)]^2}, \tag{9}$$

where

$$\alpha = \left[\frac{1}{2}(3k^4 + c^6 - c^8 - \beta_2 k^2 c^2) - k^2 c^4\right]^{1/2},$$
$$\beta = c^8 - c^6 + 4k^2c^4 - k^2\beta_2 c^2 + 3k^4\beta_2,$$
$$\gamma = 2c^2(3k^2 + c^4 - \beta_2 c^2).$$

This family of solutions contains two free parameters $c$ and $k$. It is valid when these two parameters satisfy constraint conditions $3k^4 + c^6 - c^8 - \beta_2 k^2 c^2 - 2k^2 c^4 > 0$ and $|k| > c^2$. In fact, eqs. (8) and (9) is considered as a soliton on a background whose background amplitude depends on the parameters $k$ and $c$. Figure 2 shows the

evolution behavior of MS of eq. (1) for parameters $k = 1.5$, $c = 1$, $\beta_1 = 1$, and $\beta_2 = 1$.

### 2.3 PB

Subsequently, we proceed to construct the PB of eq. (1) which should be localized in both time and space. However, as stated before, when the spatial period of ABs of eq. (1) is taken to be infinite, the amplitudes of $E(x,t)$ and $N(x,t)$ tend to zero. Here it is rather intractable to exploit the limit process to cope with PB of eq. (1) because of two free parameters. Now the approach is to directly construct the rational solution of eq. (1). The PB of eq. (1) appears

$$E(x,t) = a\mathrm{e}^{\mathrm{i}\beta_1 t}\left(\frac{4-4\mathrm{i}bt}{1+bx^2+b^2t^2}-1\right), \tag{10}$$

$$N(x,t) = \frac{4b(bx^2-b^2t^2-1)}{(1+bx^2+b^2t^2)^2}, \tag{11}$$

where $a = (1/2)\sqrt{2b(3b-\beta_2)}$. Obviously, its existence condition is the free parameter $b$ satisfy $b(3b-\beta_2) > 0$. The function $|E(x,t)|$ has the maximum amplitude $3a$ and the function $N(x,t)$ has minimum value $-4b$ at the point $(0,0)$. Here, we only consider $b > 0$ so that $\beta_2 < 3b$ to avoid the singularity in eqs. (10) and (11). The function $|E(x,0)|$ has two zeros which symmetrically locate at $x = \sqrt{3/b}$ and $-\sqrt{3/b}$. In order to achieve the higher amplitude of the function $|E(x,t)|$, the value of the parameter $b$ should be increased. Figure 3(a) shows the spatial–temporal features of the first order rational solution of eq. (1) with parameters $b = 4$, $\beta_1 = 1$, and $\beta_2 = 1$. It is interesting that the function $E(x,t)$ has bright rogue wave feature while $N(x,t)$ shows dark rogue wave feature.

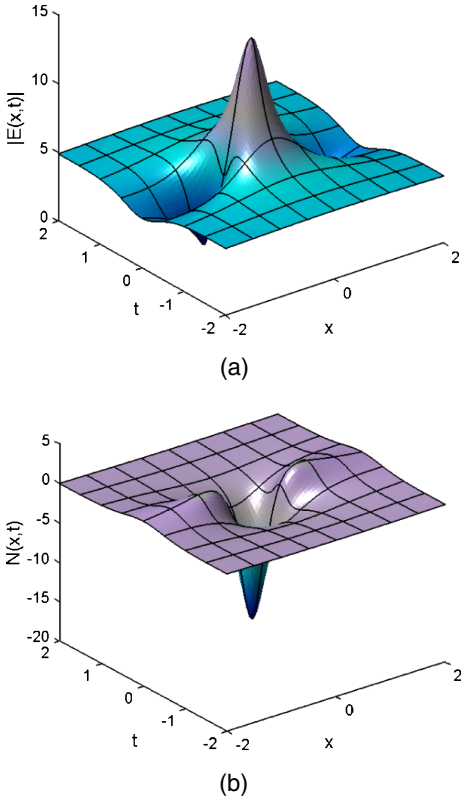


**Fig. 3.** (Color online) Spatial–temporal stucture of electric field $E(x,t)$ (a) and electrostatic potential $N(x,t)$ (b) for $b = 4$, $\beta_1 = 1$, and $\beta_2 = 1$ in the first-order rational solution (10) and (11).

To explain spectral evolution of rogue wave eqs. (10) and (11), we perform the Fourier transform:

$$F_1(\omega,t) = \frac{1}{\sqrt{2\pi}}\int_{-\infty}^{\infty} E(x,t)\mathrm{e}^{\mathrm{i}\omega x}\,\mathrm{d}x = a\sqrt{2\pi}\left[\frac{4-4\mathrm{i}bt}{2\sqrt{b(1+b^2t^2)}}\exp\left(-|\omega|\sqrt{\frac{1+b^2t^2}{b}}\right)-\delta(\omega)\right]\mathrm{e}^{\mathrm{i}\beta_1 t}, \tag{12}$$

$$F_2(\omega,t) = \frac{1}{\sqrt{2\pi}}\int_{-\infty}^{\infty} N(x,t)\mathrm{e}^{\mathrm{i}\omega x}\,\mathrm{d}x = 2b(1+2\mathrm{i})\sqrt{\frac{2b}{\pi(1+b^2t^2)}}\exp\left(-|\omega|\sqrt{\frac{1+b^2t^2}{b}}\right). \tag{13}$$

### 2.4 Second-order rational solution

Furthermore, as stated before,[18] higher-order solutions can, very likely, explain rogue waves of even higher amplitudes. Motivated by this reason, a two-parameters family of second-order rational solution yields by a proper assumption as follows

$$E(x,t) = \mathrm{e}^{\mathrm{i}\beta_1 t}\left[\frac{-6\alpha\beta_2\gamma}{s_3}+\frac{G_2(x,t)+\mathrm{i}tH_2(x,t)}{D_2(x,t)}\right], \tag{14}$$

$$N(x,t) = -2\ln[D_2(x,t)]_{xx}, \tag{15}$$

where

$$\begin{aligned}
D_2(x,t) &= \frac{s_1^2s_3^3}{\alpha^5\beta_2^3s_2^4}+\frac{s_1s_3^2s_4s_5x^2}{\alpha^3\beta_2^2s_2^4}+\frac{s_3s_6x^4}{\alpha\beta_2s_2^2}+\alpha x^6+\frac{s_3s_7t^2}{\alpha\beta_2s_2^4}+\frac{s_8\alpha^3\beta_2t^4}{s_2^2s_3}\\
&\quad+\frac{373248\alpha^7\beta_2^3t^6}{s_3^3}+\frac{s_9\alpha t^2x^2}{s_2}+\frac{216\alpha^3\beta_2t^2x^4}{s_3}+\frac{15552\alpha^5\beta_2^2x^2t^4}{s_3^2},\\
G_2(x,t) &= \frac{s_3^2s_5s_{10}s_{11}\gamma}{\alpha^4\beta_2^2s_2^4}+\frac{s_3s_{12}\gamma x^2}{\alpha^2\beta_2s_2}+\gamma x^4+\frac{s_{13}\gamma t^2}{s_2^2}+\frac{25920\gamma\alpha^4\beta_2^2t^4}{s_3^2}+\frac{432\alpha^2\beta_2\gamma t^2x^2}{s_3},\\
H_2(x,t) &= \frac{s_3s_{14}\gamma}{\alpha^2\beta_2s_2^4}-6\gamma x^2+\frac{72\alpha^2\beta_2\gamma x^4}{s_3}+\frac{s_{15}\alpha^2\beta_2\gamma t^2}{s_2^2s_3}+\frac{373248\alpha^6\beta_2^3\gamma t^4}{s_3^3}+\frac{10368\alpha^4\beta_2^2\gamma t^2x^2}{s_3^2}.
\end{aligned}$$

The coefficients $s_j$, $j = 1,2,\ldots,15$ are given by

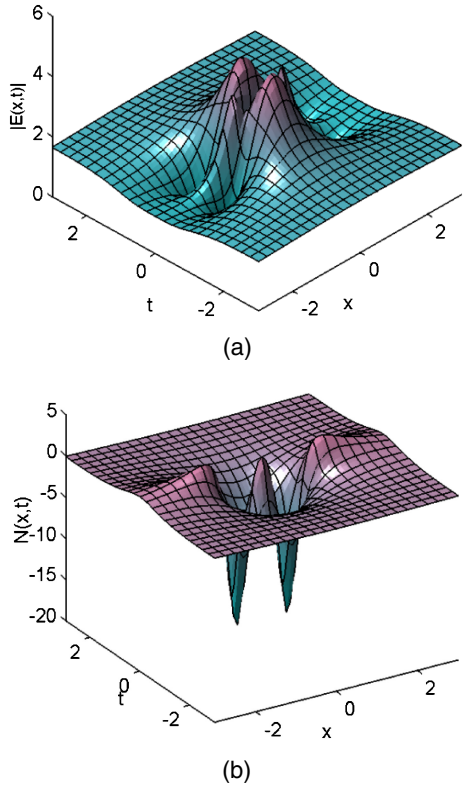


**Fig. 4.** (Color online) Spatial–temporal stucture of electric field $E(x,t)$ (a) and electrostatic potential $N(x,t)$ (b) for $\alpha = 10$, $\gamma = 50$, $\beta_1 = 1$, and $\beta_2 = 10$ in two-order rational solution (14) and (15).

$$
\begin{aligned}
s_1 &= \frac{1}{144\sqrt{2}}(129600\alpha^4 + 432\gamma^2\alpha^2 + \gamma^4),\\
s_2 &= 216\alpha^2 + \gamma^2,\\
s_3 &= 216\alpha^2 - \gamma^2,\\
s_4 &= 144\sqrt{2}(120\alpha^2 + \gamma^2),\\
s_5 &= \frac{-1}{192}(72\alpha^2 - \gamma^2),\\
s_6 &= \frac{1}{24}(129600\alpha^4 + 1584\gamma^2\alpha^2 + \gamma^4),\\
s_7 &= \frac{1}{8}(12765081600\alpha^8 + 144820224\alpha^6\gamma^2\\
&\quad + 590976\gamma^4\alpha^4 + 2592\gamma^6\alpha^2 + 11\gamma^8),\\
s_8 &= 1944(9792\alpha^4 + 176\alpha^2\gamma^2 + \gamma^4),\\
s_9 &= 18(360\alpha^2 - \gamma^2),\\
s_{10} &= 504\alpha^2 + \gamma^2,\\
s_{11} &= \frac{-1}{9}(129600\alpha^4 + 432\gamma^2\alpha^2 + \gamma^4),\\
s_{12} &= \frac{1}{12}(\gamma - 360\alpha^2),\\
s_{14} &= \frac{-1}{24}(13033820160\alpha^8 + 135862272\alpha^6\gamma^2\\
&\quad + 653184\gamma^4\alpha^4 + 3168\gamma^6\alpha^2 + 5\gamma^8),\\
s_{15} &= -144(160704\alpha^4 + 1296\alpha^2\gamma^2 - \gamma^4),\\
s_{13} &= 18(19008\alpha^4 + 48\alpha^2\gamma^2 + \gamma^4).
\end{aligned}
$$

This family of solutions involves two free parameters $\alpha$ and $\gamma$. Figure 4 shows spatial–temporal structure of second-order rational solution of eq. (1) with the parameters $\alpha = 10$, $\gamma = 50$, $\beta_1 = 1$, and $\beta_2 = 10$. It is observed the central position of this figure has a dip but not a peak compared with the second-order rational solution of NLSE. This fact indicates that the intensity in the center of rogue wave for eq. (1) is less giant than that of NLSE. To describe this dynamic behavior, we fix $\alpha = 10$, $\beta_1 = 1$, and $\beta_2 = 10$ and change the value of the parameter $\gamma$. Figure 5 shows the profile of the function $|E(x,0)|$ for several values of $\gamma$. Figures 5(a)–5(d) correspond to $\gamma = 50, 120, 130, 140$, respectively. As can be seen from the figure, the value of $|E(0,0)|$ increases and the depth of the dip decreases with $\gamma$ for the choice $0 < \gamma < 146$ to avoid the singularity. In contrast to the case of NLSE, the function $|E(x,0)|$ has no zeros and its shape is similar to the interaction between two first-order rational solutions. For higher order rational solutions, they are omitted here because of the complexity.

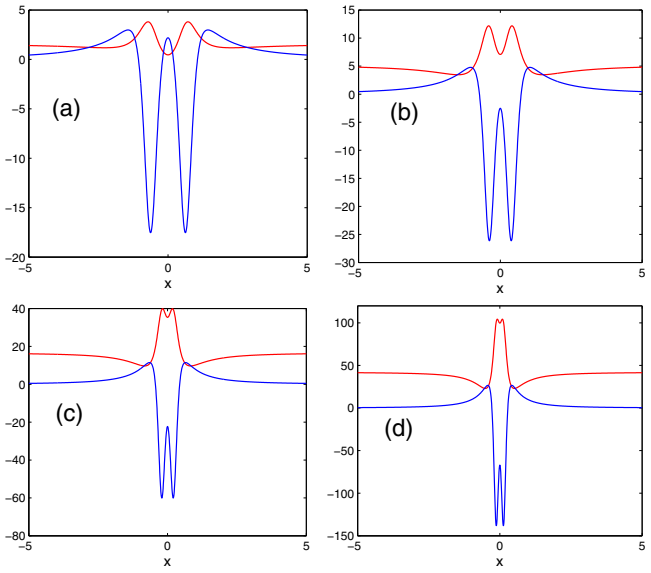


**Fig. 5.** (Color online) Plots of the function $|E(x,0)|$ (red line) and $N(x,0)$ (blue line), on the central line $t = 0$ of two-order rational solution (14), when $\alpha = 10$, $\beta_1 = 1$ and $\beta_2 = 10$ for different $\gamma$: (a) 50, (b) 120, (c) 130, and (d) 140.

## 3. Coupled Higgs Field Equation

In this section, we concentrate on that the rational solution of Higgs field equation (2) can be constructed by using Hirota technique. An equilibrium state solution of eq. (2) can be found by making the assumption

$$U = \sqrt{p_0}e^{i\omega t}, \quad V = 0, \tag{16}$$

where $\omega$ is a real constant and $p_0$ is the incident power. Plugging eq. (16) into eq. (2), we have

$$\omega^2 = p_0\beta - \alpha. \tag{17}$$

Equation (17) implies that the existence condition of solution (16) is $p_0\beta > \alpha$. By taking the following Bäcklund transformation

$$U = \frac{G}{F}, \quad V = 2(\ln F)_{xx}, \quad F \text{ real}. \tag{18}$$

(2) is transformed into the bilinear form:

$$(D_t^2 - D_x^2 + B - \alpha)G \cdot F = 0, \tag{19}$$

$$(D_t^2 + D_x^2 + B)F \cdot F - \beta G G^* = 0, \tag{20}$$

where $G^*$ is conjugate function of $G(x,t)$ and $B$ is the integration constant. Using the similar analysis with the previous section, a family of the first order rational solution of (2) results in

$$U = \sqrt{p_0}\mathrm{e}^{\mathrm{i}\omega t}\left(1 + \frac{d_3 + d_4 \mathrm{i}t}{1 + d_1 x^2 + d_2 t^2}\right),$$

$$V = \frac{4d_1(1 - d_1 x^2 + d_2 t^2)}{(1 + d_1 x^2 + d_2 t^2)^2}, \tag{21}$$

where

$$d_1 = \frac{\alpha + 3p_0\beta}{4} + \frac{\alpha(\alpha - 3p_0\beta + \chi)}{4p_0\beta} - \frac{3\chi}{4},$$

$$d_2 = \frac{3(\alpha - p_0\beta)}{4} + \frac{\alpha(\alpha - 3p_0\beta + \chi)}{4p_0\beta} - \frac{\chi}{4},$$

$$d_3 = \frac{\alpha - 3p_0\beta + \chi}{p_0\beta},$$

$$d_4 = \frac{2\alpha - 2\chi + \alpha d_3}{(p_0\beta - \alpha)^{1/2}},$$

$$\chi^2 = (\alpha + 3p_0\beta)(\alpha - p_0\beta). \tag{22}$$

This family of solutions includes a single-parameter $p_0$. Noting from eq. (22) the solution (21) is not valid in coupled Higgs field equation (2) since the conditions $\alpha \geq 0$ and $\beta > 0$ lead to $\chi^2 < 0$. When $\alpha < 0$ and $\beta < 0$ lead to $\chi^2 > 0$, this shows the rational solution (21) exist for coupled nonlinear Klein–Gordon equation. In the meantime, the rational solution (21) have singularity due to $d_1 < 0$ in this situation. However, if $\alpha < 0$ and $\beta > 0$, singularity of solution (21) will disappear. Thus, we only devote to studying this case here because rogue wave will can appear in this frame. Subsequently, the effect of parameter $\alpha$ is analyzed in eq. (2) by choosing $p_0 = 1$ and $\beta = 1$. Figures 6(a) and 6(c) illustrate the variables $d_1$ and $d_2$ in rogue wave eq. (21) as $\alpha$ ranging from $-30$ to $-3$ corresponding to $\chi > 0$ and $\chi < 0$ in eq. (22), respectively. Figures 6(b) and 6(d) show the maximum amplitudes of rogue wave $U(x,t)$ in eq. (21) as $\alpha$ corresponding to $\chi > 0$ and $\chi < 0$, respectively. It is observed the maximum magnitude of rogue wave $U(x,t)$ approaches to 5 when $\chi > 0$ while it increases linearly $\chi < 0$ as $\alpha$ becomes smaller. Hence, the maximum magnitudes of rogue wave $U(x,t)$ and $V(x,t)$ depend on the sign of $\chi$. As a result, rogue wave bifurcation occurs in this system. Figure 7 is the plots of the functions $|U(x,0)|$ and $V(x,0)$ with the parameters $\alpha = -3$ and $-10$. It can be seen that both $|U(x,0)|$ and $V(x,0)$ possess bright rogue wave. In addition, ABs and MS type solutions of the Higgs field equation (2) are also constructed by virtue of Hirota technique. However, for the sake of simplicity, they are not listed here.

## 4. Conclusion

In this work, the explicit forms of ABs, MS, PB, and the second-order rational solutions have been presented from the first up to the second of the SB equation (1). Moreover, the existence condition of rogue wave in Higgs field equation has been analyzed from the explicit form of its rational solutions. To our knowledge, these solutions are reported for the first time. In the future, whether PB of eq. (1) can be obtained by employing the limit process from MS or ABs. Besides, it is worth noting that SB equation (1) can be reduced to a coupled Schrödinger–KdV equation for unidirectional propagation.[22] Therefore, rogue wave also exists for coupled Schrödinger–KdV system. However, in the similar way, it is found that this kind of rational solutions cannot exist for the classic Zakharov system.[29–31]

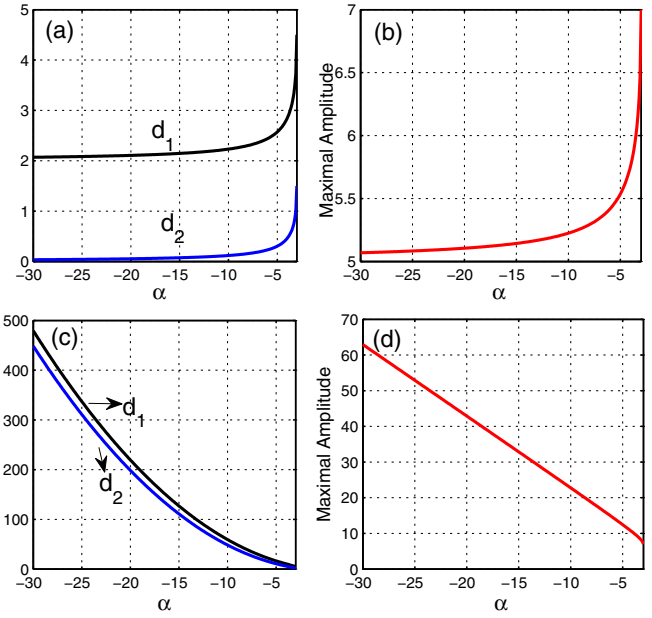


**Fig. 6.** (Color online) (a) Coefficients $d_1$ and $d_2$. (b) Maximum amplitude of $U(x,t)$ in rogue wave eq. (21) as functions $\alpha$ when $\chi > 0$ in eq. (22) with $p_0 = 1$ and $\beta = 1$. (c) and (d) correspond to $\chi < 0$ in eq. (22).

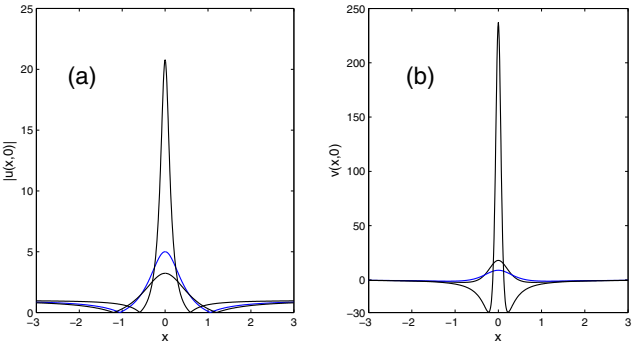


**Fig. 7.** (Color online) Plots of the functions $|U(x,0)|$ and $V(x,0)$ for $\alpha = -3$ (blue line) and $-10$ (two dark lines) with the parameters $p_0 = 1$ and $\beta = 1$ in rogue wave eq. (21).

## Acknowledgements

This work was supported by the National Natural Science Foundation of China (Nos. 10801037 and 11061028), the New Teacher Grant of Ministry of Education of China (No. 200802461007), and the Young Teachers Foundation (No. 1411018) of Fudan university. Also, the author Qin is very grateful to Professor Peter D. Miller and Professor John E. Fornaess for their enthusiastic support and useful suggestions.

1) M. Hopkin: Nature **430** (2004) 492.
2) D. I. Yeom and B. J. Eggleton: Nature **450** (2007) 953.
3) D. R. Solli, C. Ropers, P. Koonath, and B. Jalali: Nature **450** (2007) 1054.
4) C. Kharif and E. Pelinovsky: Eur. J. Mech. B **22** (2003) 603.
5) M. Onorato, A. R. Osborne, M. Serio, and S. Bertone: Phys. Rev. Lett. **86** (2001) 5831.
6) M. Onorato, A. R. Osborne, and M. Serio: Phys. Rev. Lett. **96** (2006) 014503.
7) M. S. Ruderman: Eur. Phys. J. Spec. Top. **185** (2010) 57.
8) S. W. Xu, J. S. He, and L. H. Wang: J. Phys. A **44** (2011) 305203.
9) W. M. Moslem, P. K. Shukla, and B. Eliasson: EPL **96** (2011) 25002.
10) D. H. Peregrine: J. Aust. Math. Soc., Ser. B **25** (1983) 16.
11) N. N. Akhmediev and V. I. Korneev: Theor. Math. Phys. **69** (1986) 1089.
12) V. E. Zakharov and A. I. Dyachenko: Eur. J. Mech. B **29** (2010) 127.
13) N. Akhmediev, J. M. Soto-Crespo, and A. Ankiewicz: Phys. Rev. A **80** (2009) 043818.
14) V. E. Zakharov and L. A. Ostrovsky: Physica D **238** (2009) 540.
15) V. I. Shrira and V. V. Geogjaev: J. Eng. Math. **67** (2010) 11.
16) Y. C. Ma: Stud. Appl. Math. **60** (1979) 43.
17) N. Akhmediev, J. M. Soto-Crespo, and A. Ankiewicz: Phys. Lett. A **373** (2009) 2137.
18) N. Akhmediev, A. Ankiewicz, and J. M. Soto-Crespo: Phys. Rev. E **80** (2009) 026601.
19) A. Ankiewicz, J. M. Soto-Crespo, and N. Akhmediev: Phys. Rev. E **81** (2010) 046602.
20) A. Ankiewicz, N. Akhmediev, and J. M. Soto-Crespo: Phys. Rev. E **82** (2010) 026602.
21) B. Kibler, J. Fatome, C. Finot, G. Millot, F. Dias, G. Genty, N. Akhmediev, and J. M. Dudley: Nat. Phys. **6** (2010) 790.
22) S. V. Singh, N. N. Rao, and P. K. Shukla: J. Plasma Phys. **60** (1998) 551.
23) Y. Hase and J. Satsuma: J. Phys. Soc. Jpn. **57** (1988) 679.
24) A. R. Chowdhury, B. Dasgupta, and N. N. Rao: Chaos Solitons Fractals **9** (1998) 1747.
25) X. B. Hu, B. L. Guo, and H. E. Tam: J. Phys. Soc. Jpn. **72** (2003) 189.
26) M. Tajiri: J. Phys. Soc. Jpn. **52** (1983) 2277.
27) T. Arai and M. Tajiri: Phys. Lett. A **274** (2000) 18.
28) Z. Y. Qin, G. Mu, and W. X. Ma: Int. J. Theor. Phys. **51** (2012) 999.
29) X. T. He and C. Y. Zheng: Phys. Rev. Lett. **74** (1995) 78.
30) Y. Tan, X. T. He, S. G. Chen, and Y. Yang: Phys. Rev. A **45** (1992) 6109.
31) V. E. Zakharov: Sov. Phys. JETP **35** (1972) 908.